Extending the Two-Dimensional FDTD Method to Hybrid Electromagnetic Systems with Active and Passive Lumped Elements

Wenquan Sui, Douglas A. Christensen, *Member, IEEE*, and Carl H. Durney, *Senior Member, IEEE*

Abstract—**This paper extends the finite-difference time-domain (FDTD) method to include distributed electromagnetic systems with lumped elements (a hybrid system) and voltage and current sources. FDTD equations that include nonlinear elements like diodes and transistors are derived. Calculation of driving-point impedance is described. Comparison of FDTD calculated results with analytical results for several two-dimensional transmission-line configurations illustrate the accuracy of the method. FDTD results for a transistor model and a diode are compared with SPICE calculations. The extended FDTD method should prove useful in the design and analysis of complicated distributed systems with various active, passive, linear and nonlinear lumped electrical components.**

I. Introduction

THE FDTD method, first presented by Yee in 1966 [1], numerically solves Maxwell's equations in the time domain on a spatial grid. Because of its computational efficiency, accuracy and direct physical interpretations, the FDTD method has become increasingly popular for computations of electromagnetic wave propagation and scattering problems and electromagnetic biological effects [2]–[6], including the FDTD analysis of microwave circuits [7], [8].

Previous analytical techniques for hybrid circuits (distributed electromagnetic systems with lumped elements) have used equivalent circuits or have combined different numerical methods to analyze lumped-element or semiconductor devices in a distributed system [9]–[14]. For example, for a nonuniform transmission line loaded with lumped elements equivalent transformations or equivalent circuits have been employed [11]–[13]. The transmission line matrix (TLM) method [15], [16], which simulates the wave propagation by an equivalent circuit based on Huygen's principle, is another popular numerical method. Comparisons between the FDTD and TLM methods are reported in [7], [17] and [18], with the general conclusion that the two methods, although based upon different modeling philosophies, are similar in several respects, and can be considered to be complementary; both utilize meshes and a time-domain approach. Voelker and Lomax [14] combined the TLM method with the FDTD method to gain the advantages of both methods for a semiconductor problem including both lumped elements and nonlinear devices. The TLM method has also been employed in a microwave field simulator formulated to be particularly user-friendly [19], similar to microwave circuit CAD packages which are being developed to meet the increasing demand for all-purpose CAD tools [19]–[21].

This paper extends the two-dimensional finite-difference time-domain (FDTD) numerical analysis technique to include hybrid systems, such as microwave circuits with lumped capacitors, inductors and diodes mixed with strip lines or radiating elements [22]–[25], and discrete sources with antennas such as hyperthermia applicators for cancer therapy [26]. The formulation includes calculation of driving-point impedance, which is often needed for impedance matching.

A brief review of the conventional FDTD method is followed by a derivation of the relationships between the E and H fields and the voltages and currents that are used to extend the general equations to include lumped elements inside the grid. Both R, L, and C lumped elements and discrete voltage and current sources with internal impedance are modeled; by specifying the appropriate I-V characteristics of the sources and elements, both passive and active, linear and nonlinear circuit elements, can be treated. Several test cases are analyzed by this method and the results compared with analytical solutions or the results of SPICE to verify the validity of the technique. To demonstrate the capability of the method, diodes and transistors connected to transmission lines are analyzed and the results from the extended FDTD method are compared with those from SPICE. The transmission line configurations are chosen for the comparisons because analytic solutions for these cases are easily obtained, but the method developed here applies to more complex configurations as well. Some considerations of the extended method are then discussed. Finally, prospective applications and future development of the method are discussed.

II. FDTD Formulations with Lumped Elements

Since the FDTD method has been discussed extensively in the literature [27], the two-dimensional FDTD iteration equations are stated (but not derived), and used

Manuscript received April 5, 1991; revised November 11, 1991.

The authors are with the Department of Electrical Engineering, University of Utah, Merrill Engineering Building, Salt Lake City, UT 84112.

IEEE Log Number 9106044.

as the basis for extending the method to include lumped elements. The extension is based upon the derivation of the FDTD equations from the integral form of Maxwell's equations.

A. Conventional FDTD Method

The standard FDTD equations may be derived by integrating Maxwell's equations:

$$\oint_C \vec{E} \cdot d\vec{l} = -\mu \int_S \frac{\partial \vec{H}}{\partial t} \cdot d\vec{S} \tag{1}$$

$$\oint_C \vec{H} \cdot d\vec{l} = \int_S \vec{J}_c \cdot d\vec{S} + \epsilon \int_S \frac{\partial \vec{E}}{\partial t} \cdot d\vec{S} \tag{2}$$

appropriately on a Yee cell to obtain the iteration equations:

$$H_{zi,j}^{n+1} = H_{zi,j}^{n} + \frac{\delta t}{\mu \delta l}\left(E_{xi,j+1}^{n} + E_{yi,j}^{n} - E_{xi,j}^{n} - E_{yi+1,j}^{n}\right) \tag{3}$$

$$E_{xi+1,j}^{n+1} = \frac{\dfrac{\epsilon}{\delta t} - \dfrac{\sigma}{2}}{\dfrac{\epsilon}{\delta t} + \dfrac{\sigma}{2}} E_{xi+1,j}^{n} + \frac{\dfrac{1}{\delta l}}{\dfrac{\epsilon}{\delta t} + \dfrac{\sigma}{2}} \cdot \left(H_{zi+1,j}^{n} - H_{zi+1,j-1}^{n}\right) \tag{4}$$

$$E_{yi+1,j}^{n+1} = \frac{\dfrac{\epsilon}{\delta t} - \dfrac{\sigma}{2}}{\dfrac{\epsilon}{\delta t} + \dfrac{\sigma}{2}} E_{yi+1,j}^{n} + \frac{\dfrac{1}{\delta l}}{\dfrac{\epsilon}{\delta t} + \dfrac{\sigma}{2}} \left(H_{zi,j}^{n} - H_{zi+1,j}^{n}\right). \tag{5}$$

In (3)–(5), δl is the length of a side of the square cell of the grid, ϵ is the permittivity and σ the conductivity. δt is the time interval of each iteration time step which is determined by

$$\delta t = \frac{\delta l}{F c_{\max}} \tag{6}$$

where $F \geq \sqrt{2}$ for stability in the two-dimensional problem [2] and $c_{\max}$ is the maximum speed of the electromagnetic wave inside the grid. Note that to derive (4) and (5) from (2), the E term in the current density J_c has been taken as a forward time average, i.e., $J_c^n = \sigma(E^{n+1} + E^n)/2$, to avoid an instability problem in the FDTD iteration equation when the conductivity of the medium (σ) becomes very large.

The locations and orientations of the E and H field components are shown for a typical two-dimensional unit cell of the grid (the Yee cell) in Fig. 1. We have used Mur's first-order absorbing boundary conditions [28] at the outer edges of the grid, which have been shown to provide reasonable accuracy in previous investigations [8], [26].

B. The Extended FDTD Method

Lumped elements may be accounted for in Maxwell's equations by starting with the interpretation that in (2), the right-hand side is the total integrated current density

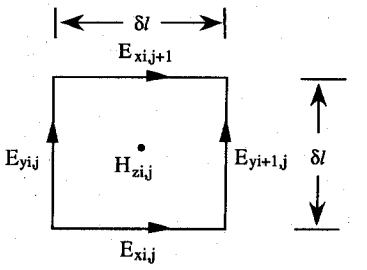

Fig. 1. Two-dimensional FDTD unit cell (Yee cell) at position (i, j).

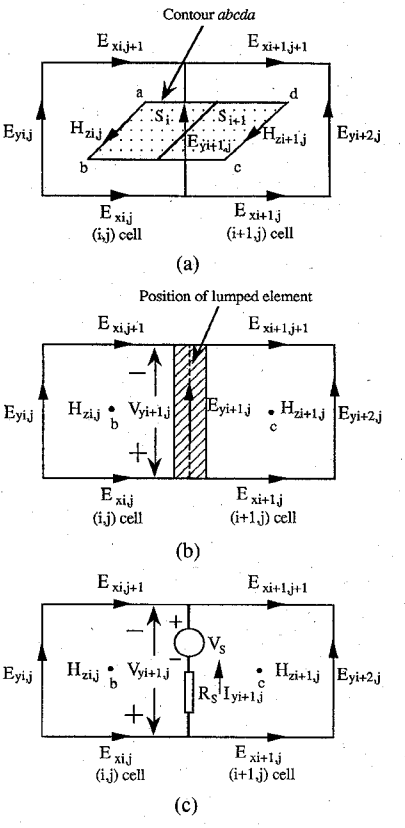

Fig. 2. Interpretation of a lumped element in an FDTD cell pair. (a) Illustration of the integral contour and field components. (b) Position of the lumped element and the related voltage. (c) Example for modeling a voltage source with internal resistor.

through a surface, which is the sum of the conduction current $\int_s J_c \cdot dS$ and the displacement current $\epsilon \int_s (\partial E/\partial t) \cdot dS$. This total current is related by (2) to the H field integrated over the corresponding contour. An example of such a contour and surface for the finite-difference formulation is shown in Fig. 2(a). The contour *abcda* is in the x-z plane. In this two-dimensional formulation, the length *ab* in the z direction is arbitrary, since all functions do not vary with z, and since the currents in the x and y directions are defined as currents per unit z length. For the contour shown in Fig. 2(a), the total current on the right-hand side of (2) is the integral of the current densities over the area of the surface between the two adjacent H-field components, shown as a shaded surface comprised of S_i and S_{i+1} in the figure. The conduction current per unit length is thus given by

$$I_{cy} = \sigma_{i,J} E_{yi+1,J} \frac{\delta l}{2} + \sigma_{i+1,J} E_{yi+1,J} \frac{\delta l}{2}$$

$$= \left(\frac{\sigma_{i,J} + \sigma_{i+1,J}}{2} \right) \delta l E_{yi+1,J}. \tag{7}$$

Note that the conduction current is proportional to the average conductivity times the electric field. Similarly, the displacement current per unit length is given by

$$I_{dy} = \left(\frac{\epsilon_{i,J} + \epsilon_{i+1,J}}{2} \right) \delta l \frac{\partial E_{yi+1,J}}{\partial t}. \tag{8}$$

The currents in (7) and (8) are currents per unit length in z, with units of A/m. Using the classical definition of potential difference of point 1 with respect to point 2,

$$V_{12} = -\int_2^1 \vec{E} \cdot d\vec{l} \tag{9}$$

we define

$$V_{yi+1,J} = \delta l E_{yi+1,J} \tag{10}$$

with the polarity as shown in Fig. 2(b). With this definition, (7) and (8) can be written as

$$I_{cy} = g_{yi+1,J} V_{yi+1,J} \tag{11}$$

$$I_{dy} = C_{yi+1,J} \frac{\partial V_{yi+1,J}}{\partial t} \tag{12}$$

where

$$g_{yi+1,J} = \frac{(\sigma_{i,J} + \sigma_{i+1,J})}{2} \tag{13}$$

$$C_{yi+1,j} = \frac{(\epsilon_{i,j} + \epsilon_{i+1,J})}{2} \tag{14}$$

are the average conductance per unit length and average capacitance per unit length, respectively. Similar relations can be written for currents in the x direction.

With these relations, (2) can be extended to include lumped elements by adding I_l, the current through the lumped element, to the right-hand side of (2). For the example shown in Fig. 2(a), this results in

$$H_{zi,J} - H_{zi+1,J} = I_y = I_{ly} + I_{cy} + I_{dy} \tag{15}$$

where I_{ly} is the current per unit length through the lumped element and I_{cy} and I_{dy} are the conduction and displacement currents per unit length as given by (11) and (12). The lumped element is assumed to be two-dimensional (no variation in the z direction) and thin enough in the x direction that it can be considered lumped, as indicated in Fig. 2(b).

When a lumped element whose current/voltage relationships are given by the general forms $I_{lx} = f_x(V_x)$ and $I_{ly} = f_y(V_y)$ is connected between cells (i, j) and $(i + 1, j)$ in Fig. 2, the finite-difference expressions (4) and (5) for those two cells become:

$$E_{xi+1,J}^{n+1} = \frac{\frac{\epsilon}{\delta t} - \frac{\sigma}{2}}{\frac{\epsilon}{\delta t} + \frac{\sigma}{2}} E_{xi+1,j}^{n} - \frac{\frac{1}{\delta l}}{\frac{\epsilon}{\delta t} + \frac{\sigma}{2}} \cdot f_x^{n+1}(E_{xi+1,J}^{n}, E_{xi+1,j}^{n-1}, \cdots, E_{xi+1,J}^{1}) + \frac{\frac{1}{\delta l}}{\frac{\epsilon}{\delta t} + \frac{\sigma}{2}} (H_{zi+1,j}^{n} - H_{zi+1,J-1}^{n}) \tag{16a}$$

$$E_{yi+1,J}^{n+1} = \frac{\frac{\epsilon}{\delta t} - \frac{\sigma}{2}}{\frac{\epsilon}{\delta t} + \frac{\sigma}{2}} E_{yi+1,J}^{n} - \frac{\frac{1}{\delta l}}{\frac{\epsilon}{\delta t} + \frac{\sigma}{2}} \cdot f_y^{n+1}(E_{yi+1,J}^{n}, E_{yi+1,J}^{n-1}, \cdots, E_{yi+1,j}^{1}) + \frac{\frac{1}{\delta l}}{\frac{\epsilon}{\delta t} + \frac{\sigma}{2}} (H_{zi,J}^{n} - H_{zi+1,J}^{n}) \tag{16b}$$

where, depending upon the functions $f_x(\cdot)$ and $f_y(\cdot)$ determined by the I-V relations of the lumped element(s) to be modeled, the above equations correspond to the finite-difference approximations to linear, integral, differential equations or their combination.

Equations (16) are general expressions for modeling any lumped element or combination of lumped elements within an FDTD cell pair. Since there is no limitation on the I-V relations of the lumped element(s), i.e., the functions $f(V)$ in (16), it appears to be possible to model any component, linear or nonlinear, in the FDTD grid.

Note that the lumped element is connected in "parallel" with the cell while the original displacement and conduction current of the cell remains; i.e., the lumped element does not replace the cell contents, since the current calculated by (15) is the *total* current, conduction current and displacement current of the medium plus the lumped-element current, flowing through the cross section enclosed by the contour *abcda* in Fig. 2. In other words, the lumped element is treated as "sizeless" compared with the cell size, which requires, of course, that the lumped element is physically small compared to a cell.

Equations (16) include two components of the function $f(\cdot)$, allowing for the possibility that the current in the lumped element has two components, namely in the x and y directions. Often one direction of the current dominates for cells connected with lumped elements.

C. Modeling of R, L, C Elements

The lumped resistor, inductor or capacitor can be modeled easily by substituting into (16) the appropriate I-V relations for each component. In finite-difference terms, these relations take the following forms (for y-directed

current) for the resistor, inductor, and capacitor, respectively:

$$I^n_{yi+1,j} = \frac{\delta l(E^{n+1}_{yi+1,j} + E^n_{(yi+1,j)})}{2R} \tag{17a}$$

$$I^n_{yi+1,j} = \frac{(\delta l)(\delta t)}{2L}\left(E^{n+1}_{yi+1,j} + 2\sum_{k=1}^{n} E^k_{yi+1,j}\right) \tag{17b}$$

$$I^n_{yi+1,j} = \frac{C\delta l}{2\delta t}(E^{n+1}_{yi+1,j} - E^{n-1}_{yi+1,j}) \tag{17c}$$

where R, L, and C are given per unit length, and zero values are assumed for both inductor current and capacitor voltage at time zero.

Forward time averages have been taken in the above equations to be consistent with the treatment of the conductance current in Section II-A. Also, if no time averaging is used for the currents, the forward-difference form of the difference equations (16) will lead to instabilities for certain values of R (we have found that a backward-difference form must be implemented to avoid instabilities if no time averaging is used).

D. Modeling of Discrete Sources

When a discrete source such as a voltage source V_s with internal series resistance R_s is included in the y direction in the cells, as shown in Fig. 2(c), the I-V relation of the branch connected with voltage source and resistor can be written as $V_y = I_y R_s - V_s$, or in finite-difference form

$$I^n_{yi+1,j} = \frac{\delta l(E^{n+1}_{yi+1,j} + E^n_{yi+1,j}) + 2V^n_s}{2R_s}. \tag{18}$$

A similar current/voltage equation can be derived for a current source I_s with an internal parallel conductance G_s.

Then substituting (18) or the corresponding equation for the current source into the FDTD iteration equation (16b) for E_y will give, respectively,

$$E^{n+1}_{yi+1,j} = \frac{\frac{\epsilon}{\delta t} - \frac{\sigma}{2} - \frac{1}{2R_s}}{\frac{\epsilon}{\delta t} + \frac{\sigma}{2} + \frac{1}{2R_s}} E^n_{yi+1,j} - \frac{\frac{V^n_s}{\delta l R_s}}{\frac{\epsilon}{\delta t} + \frac{\sigma}{2} + \frac{1}{2R_s}} + \frac{(H^n_{zi,j} - H^n_{zi+1,j})}{\left(\frac{\epsilon}{\delta t} + \frac{\sigma}{2} + \frac{1}{2R_s}\right)\delta l} \tag{19a}$$

or

$$E^{n+1}_{yi+1,j} = \frac{\frac{\epsilon}{\delta t} - \frac{\sigma}{2} - \frac{G_s}{2}}{\frac{\epsilon}{\delta t} + \frac{\sigma}{2} + \frac{G_s}{2}} E^n_{yi+1,j} - \frac{\frac{I^n_s}{\delta l}}{\frac{\epsilon}{\delta t} + \frac{\sigma}{2} + \frac{G_s}{2}} + \frac{(H^n_{zi,j} - H^n_{zi+1,j})}{\left(\frac{\epsilon}{\delta t} + \frac{\sigma}{2} + \frac{G_s}{2}\right)\delta l}. \tag{19b}$$

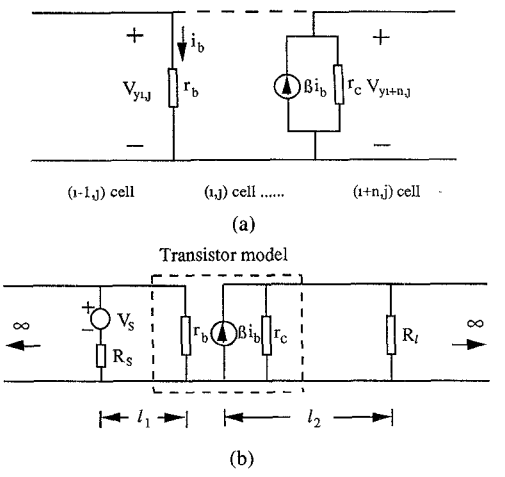

Fig. 3. Modeling of a transistor in the FDTD grid. (a) Simplified equivalent circuit of the transistor: there are n cells, $n = 1, 2, \cdots$, between the base and collector cells, as shown by the dashed line, which modifies the fringing field effect. (b) Equivalent circuit for comparisons with the SPICE calculation: the transistor (equivalent model enclosed by dashed box) is connected in an infinitely long transmission line driven by a voltage source and loaded by a resistor.

When modeling a voltage source whose internal series resistor R_s equals zero, corresponding to an ideal voltage source, the electric field is given directly from the source voltage with no need for other terms; in this case (19a) should be replaced by (10) with $V_y = -V_s$. When R_s goes to infinity, the voltage source branch becomes an open circuit, and (19a) correctly reduces to (5). Similarly, when modeling a current source, if the parallel conductance G_s goes to zero, corresponding to an ideal current source, then (19b) reduces to (16b) with $f(\cdot) = I_s$.

E. Modeling of Active and Nonlinear Devices

An active device can also be modeled by a combination of lumped elements, including dependent sources, in one or more cells inside the grid. As an example, a transistor can be modeled by the simplified equivalent circuit shown in Fig. 3(a). The base and collector of the transistor are modeled at two edges of separate cells; the collector current is driven by the base-current-controlled current source. To account for the effect of fringing fields between the base and collector in the transistor model, the distance between the base and collector may be chosen to be a varying number of cells as shown in Fig. 3(a). For more advanced modeling, lumped-element capacitors may be added in parallel to any branch.

Also, a nonlinear diode model may be included in the FDTD calculations by using the diode equation:

$$I_l = I_0(e^{qV_l/kT} - 1) \tag{20}$$

where k is Boltzmann's constant, q is the charge of an electron, T is temperature in Kelvin, and V_l is the voltage across the diode (which is related to E by (10)).

F. Calculation of Driving-Point Impedance

For any distribution system or hybrid system, the driving-point impedance Z at the source can be calculated

when the system reaches the steady state by using the following equation:

$$Z = \frac{V_0 \angle \phi_1}{I_0 \angle \phi_2} \tag{21}$$

where V_0 and I_0 are the magnitudes of the driving-point voltage and current, and ϕ_1 and ϕ_2 are their phases, for the cell that contains the excitation source, as calculated from (10) and (15).

III. Comparisons of FDTD with Transmission-Line Theory and Spice

To verify the method, we compared FDTD calculations with analytical solutions or results from SPICE for a two-ended parallel-plate transmission line with various lumped elements connected either at the source or as a load. This general configuration is chosen because analytical solutions for it are available, and because it can include the effects of multiple reflections and interference between the incident and reflected waves. Unwanted radiation into free space, which would be included in the FDTD results but which would unduly complicate the analytical analysis, are eliminated by selecting a closed transmission system.

Of the many calculations we have done, we present four that typify the agreement between FDTD results and analytical or SPICE results. The following parameters were used in the FDTD calculations: cell size was 1 cm square; all excitation signals were sinusoidal waves, $V_s(t) = V_o \sin(\omega t)$ or $I_s(t) = I_o \sin(\omega t)$, where V_o and I_o are the magnitudes of the excitations; and the frequency was 200 MHz. The separation distance between the two transmission-line plates was 2 cm (two cells) and the line was air-spaced, so the characteristic impedance of the transmission line was $Z_0 = 7.5347\ \Omega$ and only the electromagnetic TEM mode was present. The time increment used for all FDTD results was $\delta t = 16.667$ ps, according to (6) with $F = 2$. The infinitely long transmission line was simulated by placing Mur's first order absorbing boundary conditions [28] at both ends of a 200-cell long transmission line. Both the FDTD numerical computations and the SPICE simulations were done on an HP 9000 computer system. The derivations of the analytical solutions for the test models can be found in [29].

Fig. 4 shows the transmission line configuration used for several of the comparison tests. When the load Z_l in Fig. 4 is an inductor, the current through the load, as calculated by both FDTD and the analytical solution, is shown in Fig. 5. The agreement between the two methods is very good. The effect on the resulting load current from reflections between the source and load can be clearly seen; for this case the source resistance is zero.

Fig. 6 shows the excellent agreement between the FDTD calculation and SPICE calculated currents in Z_l when Z_l is a diode. For certain combinations of parameters which cause the voltage across the diode to become large, the exponential term in the diode I-V relationship wil cause instabilities in the FDTD results, apparently due to the extremely large currents involved. In such high-current cases, the exponential relationship (20) between current and voltage is no longer physically meaningful, and a modified linear I-V relationship would probably avoid the instabilities, although we have not pursued this modification.

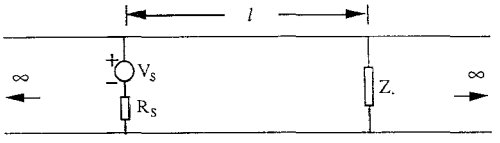

Fig. 4. One of the configurations for comparison calculations: infinite transmission line loaded by a lumped element Z_l (which can be R, L, C or diode)

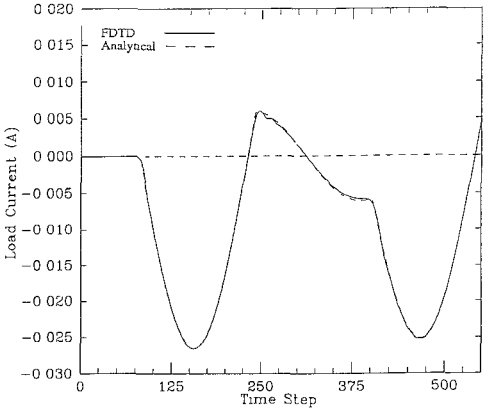

Fig. 5. Load current through L_l in Fig. 4 (inductor load) as calculated by the FDTD method (solid line) and analytical solution (dashed line) with parameters $V_0 = 1$ V, $R_s = 0\ \Omega$, $L_l = 50$ pH, and $l = 0.4$ m.

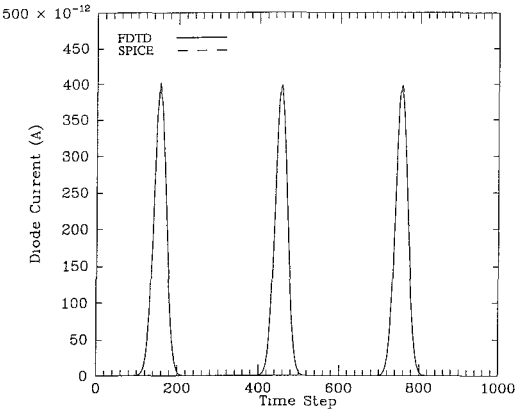

Fig. 6. Current through a diode load (Fig. 4) as calculated by the FDTD method (solid line) and SPICE simulation (dashed line) for the parameters $V_0 = 1$ V, $R_s = 0.5\ \Omega$, $l = 0.4$ m, $T = 300$ K, and $I_0 = 10^{-14}$ A. The two lines are nearly coincident.

Fig. 7 shows the FDTD results compared to SPICE calculations for the current through a load resistor in the collector/transmission-line circuit of the transistor configuration shown in Fig. 3(b). The two techniques give very similar results for the chosen set of model parameters. When the base resistance is significantly increased above the particular value chosen, however, the difference between the results of the two methods increases, probably due to an increase in the base voltage and consequent in-

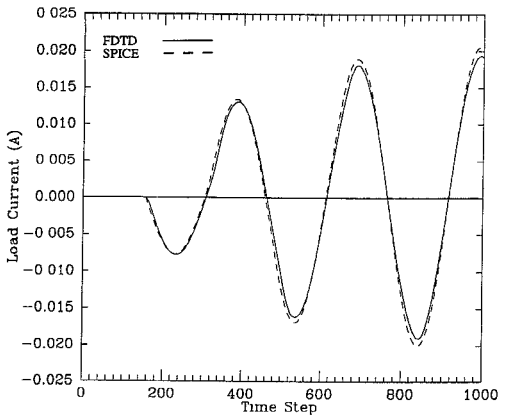

Fig. 7. Current through a load resistor in the collector circuit of a transistor-transmission line model (Fig. 3(b)) as calculated by the FDTD method (solid line) and SPICE simulation (dashed line) for the parameters V_0 = 0.1 V, R_s = 20 Ω, R_l = 2.5 Ω, β = 50, r_b = 240 Ω, r_c = 10 kΩ, l_l = 0.37 m and l_2 = 0.4 m. Also, there are three cells between the base and collector in the FDTD model.

crease in the magnitude of the fringing fields between the base and the collector; these fields are included in the FDTD analysis but not in the SPICE simulation. In a similar fashion, when the base resistance becomes very small (less than 100 Ω), the FDTD technique exhibits large instabilities, perhaps due to positive feedback via the fringing fields between the collector and base. We have placed an unphysical three-cell gap between the base and collector for the FDTD model in order to minimize the effect of the fringing fields, as indicated in Fig. 3(a), but electric field values in the region of the gap from the FDTD results show that coupling still exists. Studies using more complex models, including shielding and variable gap spacing, are needed to determine more clearly the role of fringing fields in our transistor model.

A parallel-plate transmission-line model excited by a voltage source with complex *R-L-C* impedance was also analyzed by the FDTD method. The results using (21) give a driving-point impedance value of 3.76 Ω, which is very close to the theoretical value of $Z_0/2$ = 3.7673 Ω (the factor of 2 being due to the double-ended nature of the transmission line).

IV. Discussion of Results

Calculations presented in last section show that the time-domain FDTD results are close to the analytical or SPICE results; in fact most of the curves fit each other within 1% relative error. Although our examples show only source or load currents, currents and voltages at other locations have also been checked and found to be accurate to approximately the same degree. Other configurations were tested using the method, and excellent agreement with analytical and/or SPICE results was obtained. These results illustrate the potential usefulness of the extended FDTD method for hybrid system analysis.

One interesting phenomenon we have observed during this study is the occurrence of small "early signals," i.e., the arrival of low-amplitude waves traveling at speeds faster than the actual speed of the electromagnetic waves in the transmission line. The magnitudes of these early field components are very small compared to the eventual signal strengths, and therefore they have little effect on the final results. One possible explanation of this phenomenon is that, since the selection of δt in FDTD must satisfy the stability requirement given by (6), the electromagnetic values in the numerical iterations travel twice as fast as in the real wave (when F in (6) equals 2).

Because of the half-cell offset between the E and H field components for each cell as shown in Fig. 1, the positions for calculating the analytical source current in the transmission line must also be offset by one half cell from the source position (z = 0). Ignoring the half-cell offset causes significantly larger differences between the FDTD and the analytic results. This is consistent with the interpretation in Fig. 2(b) in which the current through the surface is related to the two magnetic field components at the center of the nearby cells.

By the nature of the calculation of the current through each cell pair (Fig. 2(b)) in the FDTD technique, these currents include both the lumped-element current and the displacement current through the medium contained in the cells (and conduction current if the medium is lossy). Therefore, the displacement current due to the cell's medium must be subtracted from the total FDTD current to obtain a comparison with the analytic solution (which gives the current only through the lumped element). This displacement current is usually small, and becomes an appreciable factor only for very large impedance loads.

In this paper, the perfectly conducting metal walls of the transmission line are modeled by cells with very high conductivity in the FDTD grid. Sheen *et al* [8] simulated the perfect conductor by setting the tangential electric field components to zero and assuming the conductor to be of zero thickness. Combining the lumped-element modeling technique in this paper with Sheen's method for metal modeling may be a way to handle configurations where the thickness of the conductor layer is very small (like a microstrip line or thin film) without having to make the cell size correspondingly small.

In principle, there is no upper frequency bound for FDTD calculations as long as the cell size is kept small enough compared with the wavelength (usually one-tenth of the wavelength) to give adequate spatial resolution. The FDTD method has been used in the analysis of optical waveguides operating with frequencies higher than 10^{14}Hz [30]. From the lumped-element point of view, lumped elements have been modeled in X-band [24], [31] and recently up to 18 GHz [21].

V. Conclusion

We have developed a method for analyzing hybrid electromagnetic systems by extending the FDTD equations, and have verified its accuracy for several test cases. The extended FDTD method should prove useful in the design and analysis of complicated systems with various electri-

cal components such as active, passive, linear and nonlinear lumped elements.

The straightforward extension of this technique to three-dimensional systems is anticipated. It also seems possible to extract the *S*-parameters of the electromagnetic system by this method, or reciprocally, to analyze a system using its *S*-parameter descriptions. Implementing more complicated device models or equivalent circuits should give more accurate simulations of real systems. For example, noise sources might be included in the equivalent FDTD circuit to simulate random or thermal noise in the system to determine its noise parameters.

REFERENCES

[1] K. S. Yee, "Numerical solution of initial boundary value problems involving Maxwell's equations in isotropic media," *IEEE Trans. Antennas Propagat.*, vol. 14, no. 5, pp. 302–307, 1966.

[2] A. Taflove and M. E. Brodwin, "Numerical solution of steady-state electromagnetic scattering problems using the time-dependent Maxwell's equations," *IEEE Trans. Microwave Theory Tech.*, vol. 23, no. 8, pp. 623–630, 1975.

[3] D. M. Sullivan, D. T. Borup, and O. P. Gandhi, "Use of the finite-difference time-domain method in calculating EM absorption in human tissues," *IEEE Trans. Biomed. Eng.*, vol. 34, no. 2, pp. 148–157, 1987.

[4] J. G. Maloney *et al.*, "Accurate computation of the radiation from simple antennas using the finite-difference time-domain method," *IEEE Trans. Antennas Propagat.*, vol. 38, no. 7, pp. 1059–1068, 1990.

[5] T. Shibata *et al.*, "Analysis of microstrip circuits using three-dimensional full-wave electromagnetic field analysis in the time domain," *IEEE Trans. Microwave Theory Tech.*, vol. 36, no. 6, pp. 1064–1070, 1988.

[6] J-Y, Chen, and O. M. Gandhi, "Current induced in an anatomically based model of a human for exposure to vertically polarized EMP," *IEEE Trans. Microwave Theory Tech.*, vol. 39, no. 1, pp. 31–39, 1991.

[7] W. K. Gwarek, "Analysis of arbitrarily shaped two-dimensional microwave circuits by finite-difference time-domain method," *IEEE Trans. Microwave Theory Tech.*, vol. 36, no. 4, pp. 738–744, 1988.

[8] D. M. Sheen *et al.*, "Application of the three-dimensional finite-difference time-domain method to the analysis of planar microstrip circuits," *IEEE Trans. Microwave Theory Tech.*, vol. 38, no. 7, pp. 849–857, 1990.

[9] K. Kobayashi *et al.*, "Equivalent transformations for mixed-lumped and multiconductor coupled circuits," *IEEE Trans. Microwave Theory Tech.*, vol. 30, no. 7, pp. 1034–1041, 1982.

[10] D. Winklestein *et al.*, "Simulation of arbitrary transmission line networks with nonlinear terminations," *IEEE Trans. Circuits Syst.*, vol. 38, no. 4, pp. 418–422, 1991.

[11] K. Kobayashi *et al.*, "Kuroda's identity for mixed lumped and distributed circuits and their application to nonuniform transmission lines," *IEEE Trans. Microwave Theory Tech.*, vol. 29, no. 2, pp. 81–86, 1981.

[12] I. Endo *et al.*, "Design of transformerless quasi-broad-band matching networks for lumped complex loads using nonuniform transmission lines," *IEEE Trans. Microwave Theory Tech.*, vol. 36, no. 4, pp. 629–634, 1988.

[13] Y. Nemoto *et al.*, "Equivalent transformations for the mixed lumped Richards section and distributed transmission line," *IEEE Trans. Microwave Theory Tech.*, vol. 36, no. 4, pp. 635–641, 1988.

[14] R. H. Voelker and R. J. Lomax, "A finite-difference transmission line matrix method incorporating a nonline device model," *IEEE Trans. Microwave Theory Tech.*, vol. 38, no. 3, pp. 302–312, 1990.

[15] P. B. Johns and R. L. Beurle, "Numerical solution of 2-dimensional scattering problems using transmission-line matrix," *Proc. Inst Elec. Eng.*, vol. 118, no. 9, pp. 1203–1208, 1971.

[16] W. J. R. Hoefer, "The transmission-line matrix method--theory and applications," *IEEE Trans. Microwave Theory Tech.*, vol. 33, no. 10, pp. 882–893, 1985.

[17] P. B. Johns, "On the relationship between TLM and finite-difference methods for Maxwell's equations," *IEEE Trans. Microwave Theory Tech.*, vol. 35, no. 1, pp. 60–61, 1987.

[18] W. K. Gwarek and P. B. Johns, "Comments on 'On the relationship between TLM and finite-difference methods for Maxwell's equations," *IEEE Trans. Microwave Theory Tech.*, vol. 35, no. 9, pp. 872–873, 1987.

[19] P. P. M. So *et al.*, "A two-dimensional transmission line matrix microwave field simulator using new concepts and procedures," *IEEE Trans. Microwave Theory Tech.*, vol. 37, no. 12, pp. 1877–1884, 1989.

[20] R. H. Jansen *et al.*, "A comprehensive CAD approach to the design of MMIC's up to MM-wave frequency," *IEEE Trans. Microwave Theory Tech.*, vol. 36, no. 2, pp. 208–219, 1988.

[21] E. Pettenpaul *et al.*, "CAD models of lumped elements on GaAS up to 18GHz," *IEEE Trans. Microwave Theory Tech.*, vol. 36, no. 2, pp. 294–304, 1988.

[22] R. J. Hwu *et al.*, "Array concepts for solid-state and vacuum microelectronics millimeter-wave generation," *IEEE Trans. Electron Devices*, vol. 36, no. 11, pp. 2645–2650, 1989.

[23] C. F. Jou *et al.*, "Millimeter-wave diode-grid frequency doubler," *IEEE Trans. Microwave Theory Tech.*, vol. 36, no 11, pp. 1507–1514, 1988.

[24] M. Caulton *et al.*, "Status of lumped elements in microwave integrated circuits-Present and future," *IEEE Trans. Microwave Theory Tech.*, vol. 19, no. 7, pp. 588–599, 1971.

[25] R. Levy, "A new class of distributed prototype filters with applications to mixed lumped/distributed component design," *IEEE Trans. Microwave Theory Tech.*, vol. 18, no. 12, pp. 1064–1071, 1970.

[26] J. A. Shaw, C. H. Durney, and D. A. Christensen, "Computer-aided design of two-dimensional electric-type hyperthermia applicators using the finite-difference time-domain method," *IEEE Trans. Biomed. Eng.*, vol. 38, no. 9, pp. 861–870, 1991.

[27] A. Taflove, "The FDTD method for numerical modeling of EM wave interactions with arbitrary structures," in *Electromagnetics Research, Part 2· Progress in Electromagnetics Research*, J. A. Kong Ed., Elsevier, New York, 1990, ch. 8.

[28] G. Mur, "Absorbing boundary conditions for the finite-difference approximation of the time-domain electromagnetic-field equations," *IEEE Trans. Electromagn. Compat.*, vol. 23, no. 4, pp. 377–382, 1981.

[29] W. Sui, "An extended finite difference time domain method for hybrid electromagnetic systems with active and passive lumped elements," Master's thesis, Electrical Engineering Department, University of Utah, June 1991.

[30] D. Christensen *et al.*, "Evanescent-wave coupling of fluorescence into guided modes: FDTD analysis," *SPIE*, vol 1172, Chemical, Biochemical, and Environmental Sensors, pp. 70–74, 1989.

[31] C. S. Aitchison *et al.*, "Lumped-circuit elements at microwave frequencies," *IEEE Trans. Microwave Theory Tech.*, vol. 19, no. 12, pp. 928–937, 1971.

Wenquan Sui, photograph and biography not available at the time of publication.

Douglas A. Christensen (M'69), photograph and biography not available at the time of publication.

Carl H. Durney (S'60-M'64-SM'80), photograph and biography not available at the time of publication.